

Supplementary Information

HCl and O₂ co-activated bis(8-quinolinolato) oxovanadium(IV) complexes as efficient photoactive species for visible light-driven oxidation of cyclohexane to KA oil

Jialuo She,^a Xiangfeng Lin,^b Zaihui Fu,^{*b} Jianwei Li,^{*a} Senpei Tang,^b Ming Lei,^a Xin Zhang,^a Chao Zhang,^b and Dulin Yin^b

^aState Key Laboratory of Chemical Resource Engineering, Beijing University of Chemical Technology, Beijing 100029, P. R. China

^bNational & Local United Engineering Laboratory for New Petrochemical Materials & Fine Utilization of Resources, Key Laboratory of Resource Fine-Processing and Advanced Materials of Hunan Province and Key Laboratory of Chemical Biology and Traditional Chinese Medicine Research (Ministry of Education of China), College of Chemistry and Chemical Engineering, Hunan Normal University, Changsha 410081, P. R. China

Experimental methods

The major methods here were the same as that in the main text. Please see below for more details.

Details of DFT calculations

DFT calculations were performed by using Gaussian 09 D.01 software package.¹ Geometry optimizations and Born-Oppenheimer electronic energies (including nuclear repulsion) were calculated by the empirical hybrid meta-GGA density functional M06.² The 6-31+G(d,p) basis set (Pople-type) was adopted for main group elements and pseudopotential basis set^{3,4} LANL2TZ augmented with an f-type polarization function,⁵ denoted as LANL2TZ(f),⁶ was adopted for vanadium. The parameters of LANL2TZ(f) were downloaded from the EMSL Basis Set Library.⁷ Ultrafine integration grids⁸ without symmetry constrains are used in all the calculations. The frequency evaluations were further performed to confirm the nature of the local minima in the potential energy surface. Bulk solvent effects of the MeCN medium were calculated by the polarizable continuum model (PCM) through the SCRF method.⁹ The natural bond orbital (NBO) analysis¹⁰ based on optimized geometries was conducted by using NBO Version 3.1, and thus the obtained natural charges and Wiberg bond indexes (WBIs) were used to analyze the key reaction species and their interactions with HCl. In study of the multi-HCl-interacted species, we followed the rule that every initial structure was based on the previous optimized one by adding one HCl that was in its free state in MeCN. Since hundreds of isomers, in whole, could be generated if up to three HCl molecules was added, only the isomers with the lowest Gibbs free energies (G_{298} , at 298 K in MeCN) in the same species were screened out and listed in this supplementary data. Additionally, the stablest isomers with different 8-quinolinolato ligands in the same species usually have very similar structures, so only the representative structures drawn by GaussView 5.0 were shown here unless mentioned otherwise.

* Corresponding author. Tel.: +86 731 88872576; Fax: +86 731 88872531.
E-mail address: fzhhnu@126.com

* Corresponding author. Tel.: +86 731 88872576; Fax: +86 731 88872531.
E-mail address: fzhhnu@126.com

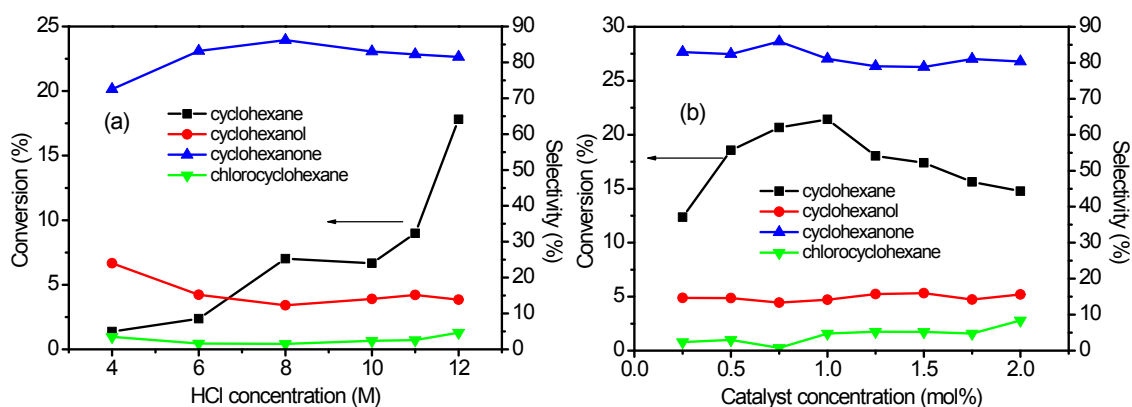


Fig. S1 The influence of HCl concentration (in 0.1 mL water, (a)) and catalyst dosage (based on substrate, (b)) on the cyclohexane (1 mmol) oxidation photocatalyzed by $V^{IV}O(Q_c)_2$ under O_2 .

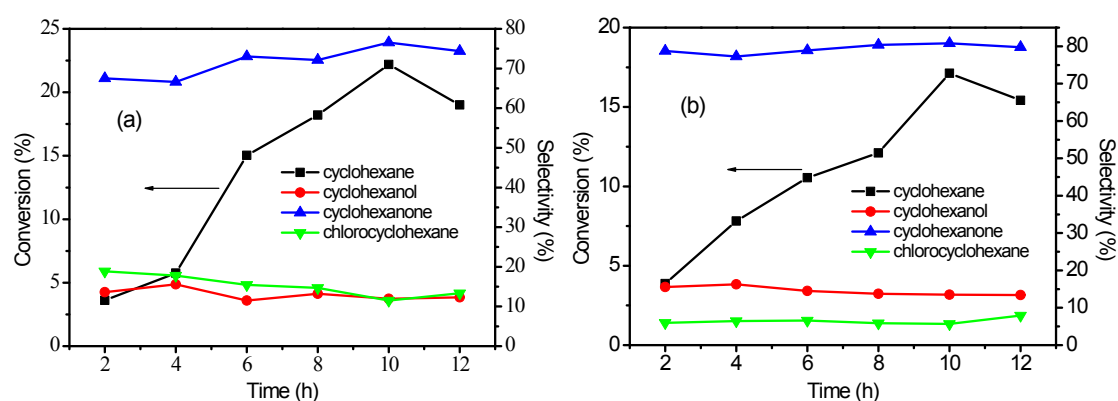


Fig. S2 The time-dependency of conversion and selectivity in the oxidation of cyclohexane (1 mmol) by O_2 with 0.01 mmol catalysis ($V^{IV}O(Q_b)_2$ (a) and $V^{IV}O(Q_c)_2$ (b)) in 5.0 mL MeCN containing 0.1 mL conc. HCl aq. under light.

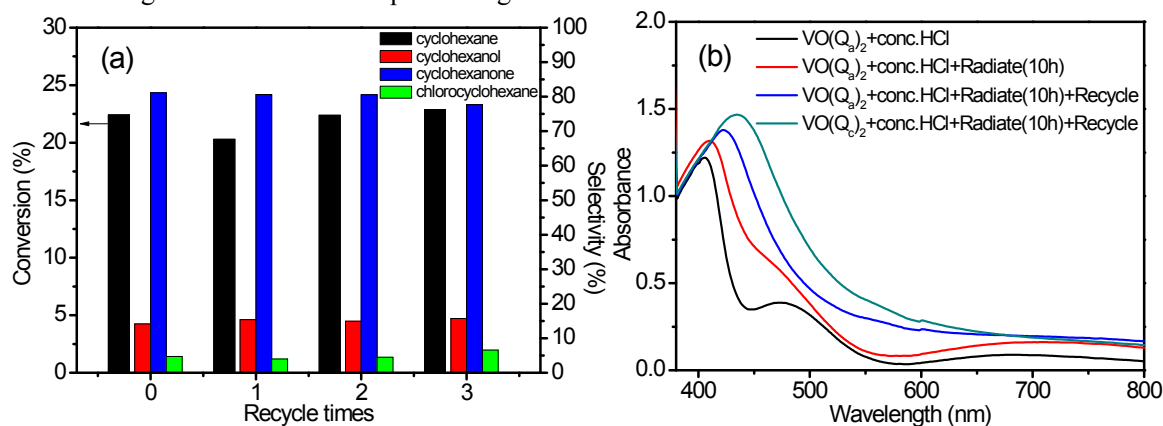


Fig. S3 The reusability of $V^{IV}O(Q_c)_2$ (a) and the visible spectra (b) before and after the recycling tests in the reaction concentration of the catalyst.

The used catalysts ($V^{IV}O(Q_a)_2$ and $V^{IV}O(Q_c)_2$) were recycled by the vacuum-rotary evaporation (50°C). The latter was applied to the reusability test. Because of the low dose in solution, this catalyst was recycled without analyzing the product composition by GC until the specific round of test was met. In each round, the cyclohexane conversion and the KA oil selectivity were maintained at about 20% and 95%, respectively. In the last round, the KA oil selectivity was declined slightly to 93.5% due to the inevitable small losses of ligands during the recycling process.

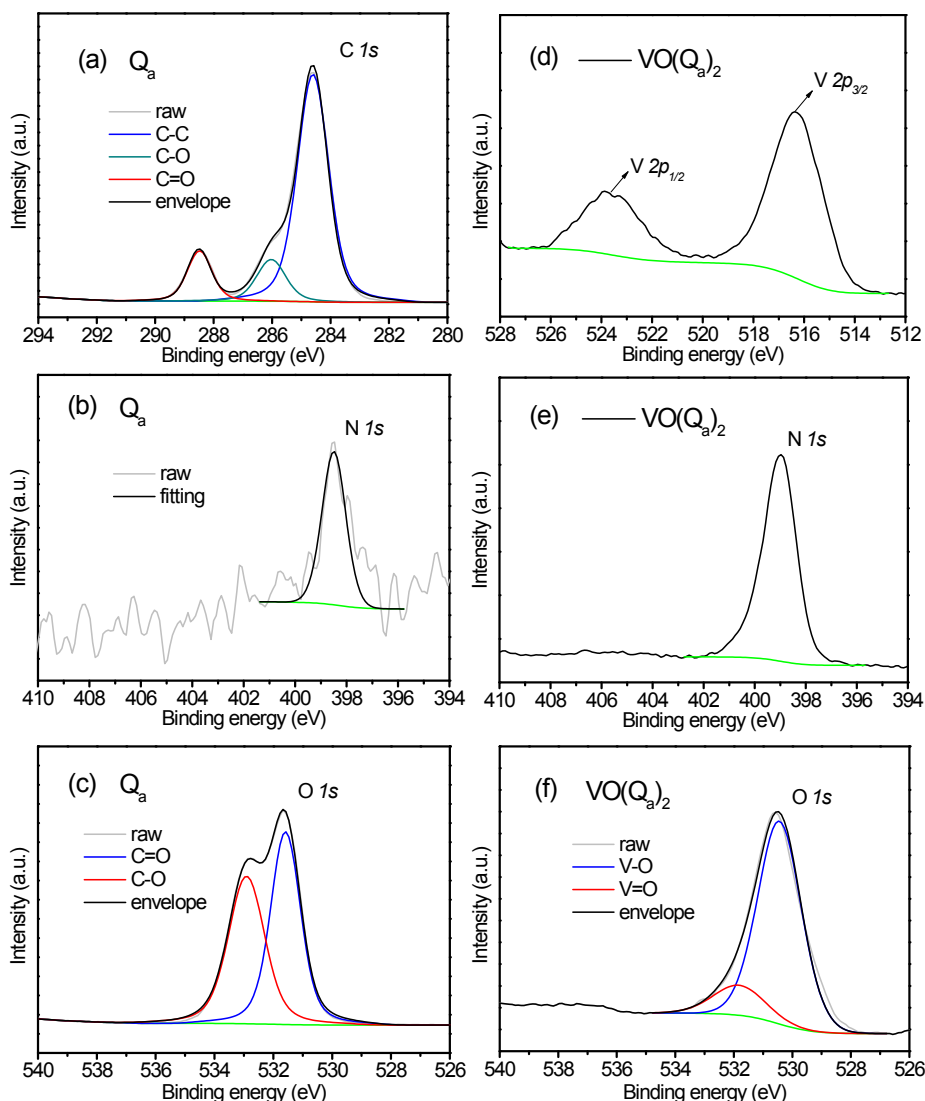


Fig. S4 The XPS *C 1s* (a), *N 1s* (b), *O 1s* (c) spectra of Q_a , and the *V 2p* (d), *N 1s* (e) and *O 1s* (f) spectra of $V^{IV}O(Q_a)_2$.

Usually the *C 1s* binding energy (BE) of C-C group in aromatic ring is assigned to 284.6 eV.¹¹ This value can be increased by halogenations effect, for example, the average value of primary (C-Cl) or secondary (the C near C-Cl) chemical shift upon chlorination is 1.5 or 0.3 eV, respectively.¹¹ The arithmetic average of this value in Qc is 0.43 eV according to its structure. Although this mean value can be further increased in view of the O and N within Qc, it is reasonable to use 0.4 eV to adjust this BE of *C 1s*. Because the *C 1s* mean values of various groups are not accurate enough to define the specific ligand (Qc), and moreover the BEs of *N 1s*, *O 1s* and *V 2p* are basically consistent with those in the reported V^{IV} -complexes containing V-N, V-O-C and V=O after this adjustment.^{12,13} Therefore, all the discussions are based on the above adjustments. Strangely, though the element contents of Q_a were in good agreement with the theoretical values (not list here), its *N 1s* peak was quite weak ((b) vs. (e)). Particularly, the prominent characteristic peaks concerning C=O respectively arose in the spectra of *C 1s* and *O 1s* ((a) and (c)), although this group was not in its structural formula. Moreover, the peak area of C=O species was approached that of C-O in above spectra. Those unusual findings were affirmed by the repeated measurements, and can be rational by the explanation that plenty of hydrogen bonds between Q_a

molecules were formed and exposed to the surface of the sample, weakening the signal of N *1s*. $V^{IV}O(Q_a)_2$ was in reduction state after the coordination ($V\ 2p_{3/2} = 516.4\ \text{eV}$, (d)). The electron donation from N *2p* to V *3d* (N *1s*: $398.5 \rightarrow 399.0\ \text{eV}$) and the back donation from V *3d* to O *2p* (O *1s*: $532.9 \rightarrow 530.4\ \text{eV}$) were coexistent in it ((b) vs. (e), (c) vs. (f)). The O atom in V-O preferred to be protonized compared to that in V=O (BE: $530.4\ \text{vs.}\ 531.8\ \text{eV}$, (f)).

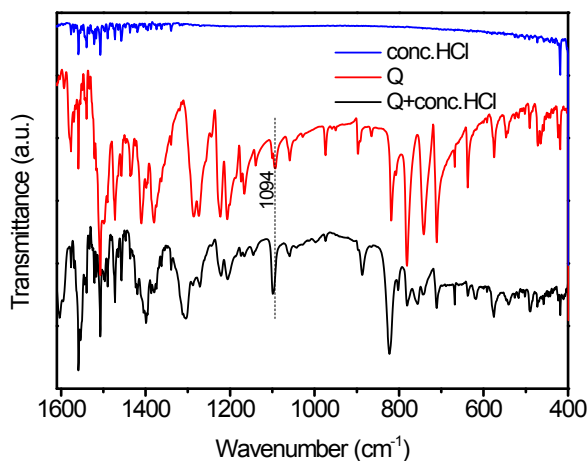


Fig. S5 FT-IR spectra of 8-hydroxyquinoline (ligand Q_a) with and without HCl.

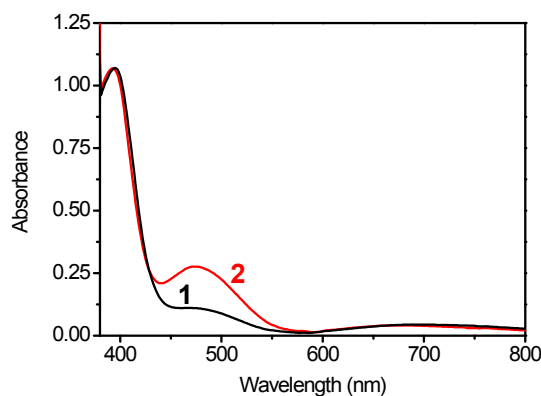


Fig. S6 Liquid visible spectra of $V^{IV}O(Q_a)_2$ in double diluted MeCN solution with 1-fold catalyst amount, and 1-fold (1) or 1.6-fold (2) conc. HCl, respectively, compared to reaction concentration.

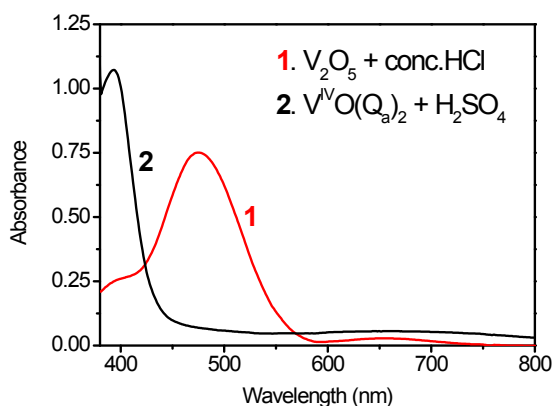


Fig. S7 Liquid visible spectra of V_2O_5 -HCl aq. (1) and $V^{IV}O(Q_a)_2$ - H_2SO_4 (2) systems. Such two MeCN solutions (5 mL) contained 5×10^{-3} mmol V element and 0.6 mmol H^+ of Bronsted acid.

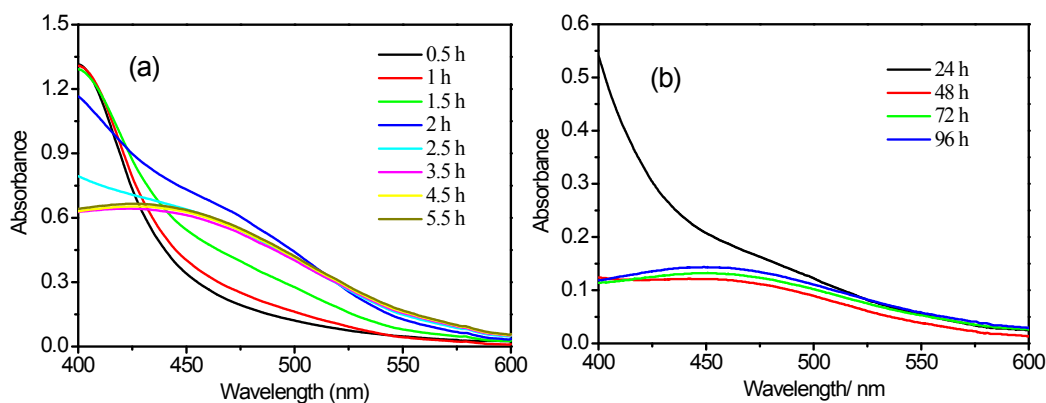


Fig. S8 Liquid visible spectra of $V^{IV}O(Q_a)_2$ (0.01 mmol) in MeCN mixed solutions (5 mL) treated with 30% H_2O_2 (20 vol.%, 35°C, (a)) and O_2 (60 vol.% THF, 80°C, (b)), respectively.

The methods to obtain the in-situ generated vanadium(V)-oxo-monoperoxo species $V^VO(O_2)$ were described in the caption of Fig. S8 and confirmed by other researchers.^{14,15} Both of the characteristic bands were centered near 450 nm, which were in the common range (400–450 nm) of $V^VO(O_2)$.¹⁴ Notably, when using O_2 to synthesize the species $V^VO(O_2)$, a much longer time and higher temperature were necessary.

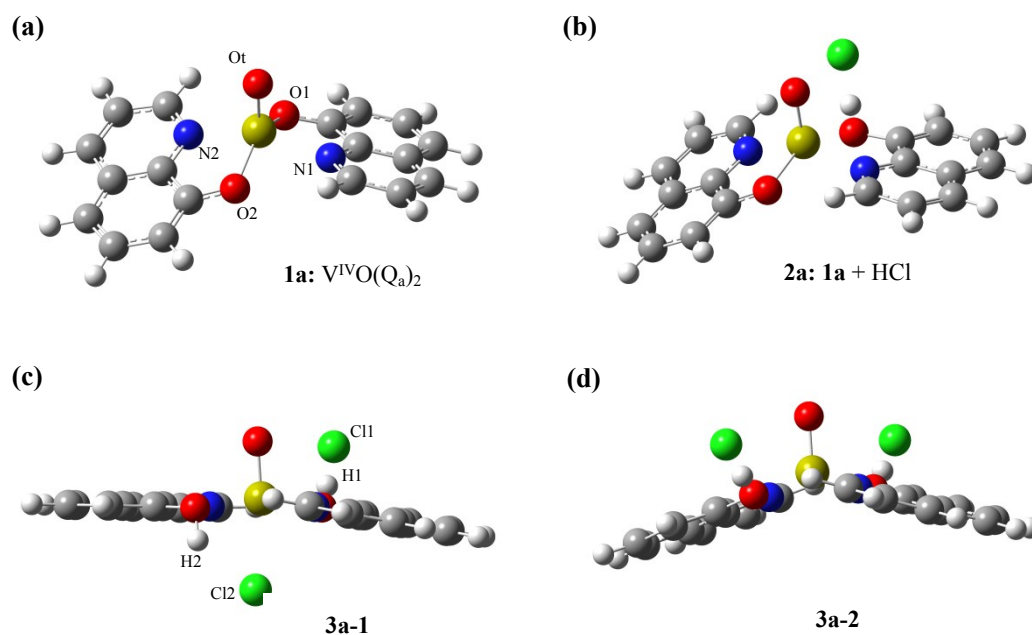


Fig. S9 Optimized geometries of species **1a** (a), one HCl-interacted **1a** (**2a**, (b)) and two HCl-interacted **1a** (its Cl-axial mode **3a-1** (c) and Cl-nonaxial mode **3a-2** (d)).

In each subfigure, the bridging $O_b(2)$ atom of cleaved V- O_b bond (being intact in **1a**) was placed in front of the reader. The serial numbers of N and O_b are identical to each other in the same ligand. Moreover, other species are also submitted to such naming rules hereinbelow. The marking colors of elements: white, grey, blue, red, green and dark yellow balls represented hydrogen, carbon, nitrogen, oxygen, chlorine and vanadium atoms, respectively. This marking rule is applied to other figures.

Table S1 The Wiberg bond indexes (WBIs) and natural charges in species **1** and MeCN-axially coordinated species **1** in MeCN medium.

Species	WBIs					Natural charges			
	V-N(1)	V-N(2)	V-O _b (1)	V-O _b (2)	V=O _t	V	N	O _b	O _t
1a	0.462	0.462	0.614	0.614	2.108	1.020	-0.460	-0.682	-0.506
1b	0.458	0.458	0.611	0.611	2.116	1.024	-0.457	-0.678	-0.490
1c	0.459	0.459	0.595	0.595	2.133	1.032	-0.460	-0.668	-0.475
1a + MeCN ^a	0.466	0.466	0.580	0.580	2.152	0.866	-0.439	-0.672	-0.463
1b + MeCN ^a	0.463	0.463	0.576	0.576	2.162	0.860	-0.437	-0.664	-0.452
1c + MeCN ^a	0.464	0.464	0.561	0.560	2.179	0.851	-0.436	-0.652	-0.435

^a one MeCN-coordinated V^{IV}OQ₂ complexes

Table S1 shows that the WBIs of V-O_b or V-N bonds are almost the same for both ligands in each V^{IV}OQ₂ complex, also, the WBIs of V-O_b, V-N or V=O bonds are only slightly different among these complexes. The O_b atoms possess the strongest protonated ability in each complex, and such ability can be weakened by substituting Cl into the ligands.

When one acetonitrile (MeCN) molecule coordinates to species **1** axially, the positive charge (PC) of V and the negative charges (NC) of N and O_t decrease significantly, which enhance the selectivity of O_b in the protonation with HCl. However, evaluating the interaction between Cl-axial species and a single MeCN is difficult. Thus only bulk solvent effects of MeCN were taken into account in the following calculations, although the comparability of V charges, between the species with vacant and occupied axial-site, was weakened.

Table S2-1 The WBIs in HCl-interacted species **1** in MeCN.

Species	WBIs								
	V-N(1)	V-N(2)	V-O _b (1)	V-O _b (2)	O _b (1)-H(1)	O _b (2)-H(2)	H-Cl(1)	H-Cl(2)	V-Cl(2)
2a	0.471	0.485	0.384	0.663	0.458		0.256		
2b	0.466	0.480	0.387	0.659	0.446		0.277		
2c	0.469	0.474	0.400	0.637	0.370		0.393		
3a-1	0.469	0.471	0.443	0.348	0.435	0.613	0.291	0.021	0.617
3b-1	0.466	0.466	0.452	0.343	0.409	0.611	0.334	0.021	0.630
3c-1	0.455	0.466	0.475	0.304	0.329	0.622	0.458	0.008	0.672
3a-2	0.492	0.492	0.433	0.433	0.406	0.405	0.342	0.342	
3b-2	0.485	0.485	0.440	0.440	0.379	0.379	0.386	0.386	
3c-2	0.472	0.480	0.415	0.583	0.351	0.061	0.424	0.829	

2a–2c and **3a–3c** indicate the one and two HCl-interacted species **1a–1c**, respectively. Notably, the species with tab “-1” represent Cl-axially coordinated mode, i.e. species from **3a-1** to **3c-1**, and the tab “-2” mean Cl-nonaxial mode similarly. The WBI of free HCl is 0.896 in MeCN. The H-Cl(1) and H-Cl(2) represent the first and the second HCl, respectively.

Table S2-2 The natural charges in HCl-interacted species **1** in MeCN.

Species	Natural charges									
	V	N(1)	N(2)	O _b (1)	O _b (2)	O _t	H(1)	H(2)	Cl(1)	Cl(2)
2a	1.060	-0.472	-0.475	-0.725	-0.668	-0.447	0.521			-0.794
2b	1.066	-0.470	-0.473	-0.725	-0.665	-0.432	0.514			-0.779
2c	1.059	-0.467	-0.475	-0.731	-0.657	-0.421	0.469			-0.688
3a-1	0.731	-0.437	-0.445	-0.701	-0.690	-0.363	0.508	0.583	-0.773	-0.553
3b-1	0.723	-0.433	-0.439	-0.700	-0.690	-0.353	0.491	0.584	-0.740	-0.542
3c-1	0.712	-0.431	-0.437	-0.702	-0.679	-0.355	0.443	0.585	-0.645	-0.516
3a-2	1.101	-0.484	-0.484	-0.725	-0.725	-0.383	0.489	0.489	-0.728	-0.728
3b-2	1.101	-0.478	-0.478	-0.726	-0.726	-0.381	0.471	0.471	-0.694	-0.693
3c-2	1.055	-0.470	-0.474	-0.729	-0.693	-0.401	0.456	0.321	-0.663	-0.352

The natural charges of H and Cl atoms in HCl are ± 0.327 , respectively.

Tables S2-1 and S2-2 list the WBIs and natural charges for one to two HCl-interacted V^{IV}OQ₂ complexes. One HCl interaction mode shows an obvious decrease in the WBI of one V-O_b(1) bond in each complex but a slight increase in another V-O_b(2) bond, along with an increase of V-N(1) and especially V-N(2) bonds. Meanwhile, the WBI of the H-Cl bond itself decreases drastically. Also, the negative charges (NC) of two N and especially O_b(1) atoms increase, and the latter's NC reach the maximum under this condition. Additionally, the H and Cl atoms of HCl respectively show more positive charge (PC) and NC when the HCl molecules interact with these complexes.

The Cl-axial mode is of interest among the two HCl interaction modes. In this mode, compared with one HCl mode, adding the second HCl can obviously decrease the WBI of the V-O_b(2) bond but slightly increase the WBI of the V-O_b(1), along with a slight decrease in the WBI of two V-N bonds. Additionally, the WBI of the H-Cl(2) is drastically reduced to nearly zero, which corresponds to the existence of the V-Cl(2) bond (WBI > 0.6), along with the significant decrease in the PC of V and the NC of Cl(2).

Table S3 The ΔG_{298} between two kinds of coordination modes of species **3** in MeCN.

Species	Without axis-MeCN		With axis-MeCN	
	G ₂₉₈ /a. u.	ΔG_{298} /kcal.mol ⁻¹	G ₂₉₈ ^a /a. u.	ΔG_{298} /kcal.mol ⁻¹
3a-1	-2020.544092	4.091	-2153.197619	-0.636
3a-2	-2020.550611		-2153.196606	
3b-1	-2939.693545	2.193	-3072.347072	-1.044
3b-2	-2939.697039		-3072.345408	
3c-1	-3858.834691	6.125	-3991.488218	0.041
3c-2	-3858.844452		-3991.488284	

^a G₂₉₈ of the species with axis-MeCN or free MeCN molecule. G₂₉₈(MeCN) = -132.653527 a.u.

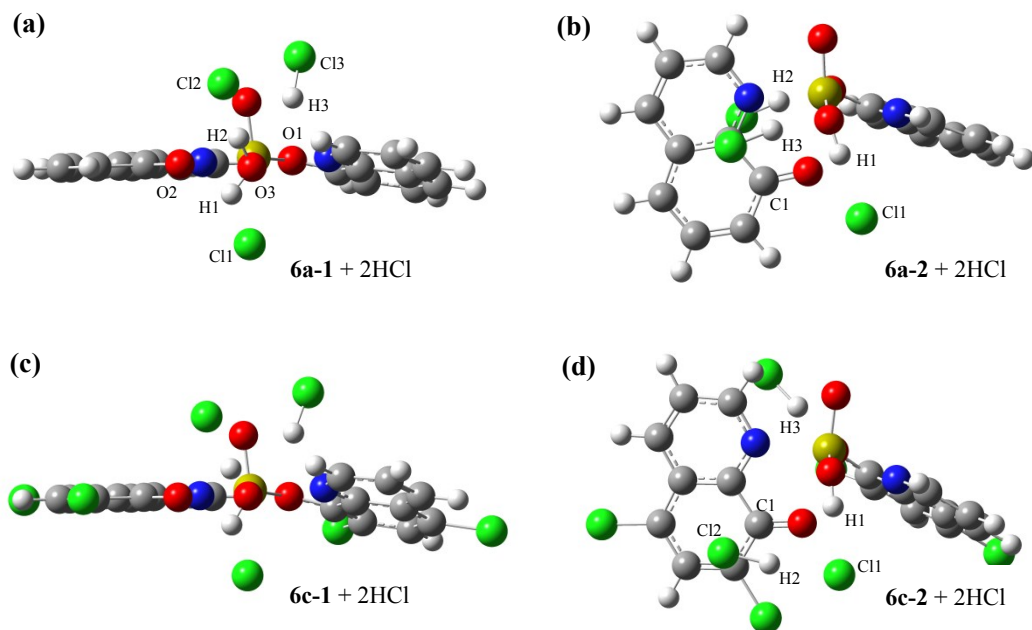


Fig. S10 Typical geometries of species **6** interacting with two HCl respectively in their Cl-axial and Cl-nonaxial modes, such species with ligand Q_a for **6a-1** + 2HCl (a) and **6a-2** + 2HCl (b), and with Q_c for **6c-1** + 2HCl (c) and **6c-2** + 2HCl (d).

In each subfigure, the O atoms with larger serial numbers (except for O_i) were placed in front of the reader, i.e. the one in V-O(3)H and another one in cleaved V-O_b(2) bond. Besides, other species are also submitted to such naming rules hereinbelow unless mentioned otherwise.

Noteworthy, the behaviours of two extra-interacted HCl in **6c-2** + 2HCl are interesting, since the first one tends to form a hydrogen bond with the Cl anion belonging to this species and the second one is slightly sloping upwards above the surface of the ligand containing $O_b(1)$.

Table S4-1 The WBIs in Cl-axially and Cl-nonaxially coordinated species **6** in MeCN.

Species	WBIs							
	V-N(1)	V-N(2)	V-O _b (1)	V-O _b (2)	V-O(3)	O(3)-H(1)	H-Cl(1)	V-Cl(1)
6a-1	0.496	0.368	0.754	0.361	1.014	0.684	0.001	0.603
6a-2	0.516	0.473	0.761	0.270	1.281	0.573	0.128	0.017
6b-1	0.487	0.359	0.741	0.369	1.023	0.684	0.001	0.618
6b-2	0.511	0.470	0.754	0.277	1.291	0.575	0.132	0.018
6c-1	0.489	0.351	0.699	0.349	1.050	0.684	0.002	0.655
6c-2	0.515	0.477	0.717	0.269	1.308	0.566	0.143	0.019

The O(3) atom belongs to the V^V(OH) group. The H-Cl(1) belongs to the core layer of species **6** (Fig. 8 vs. S10), however it came from the H-Cl(2) listed in Table S2-1 according to Scheme 1.

Table S4-2 The natural charges in Cl-axially and Cl-nonaxially coordinated species **6** in MeCN.

Species	Natural charges									
	V	N(1)	N(2)	O _b (1)	O _b (2)	O(3)	O _t	H(1)	Cl(1)	HCl(1)
6a-1	0.666	-0.381	-0.376	-0.579	-0.509	-0.788	-0.310	0.531	-0.559	-0.028
6a-2	0.871	-0.430	-0.417	-0.587	-0.518	-0.698	-0.323	0.530	-0.895	-0.365
6b-1	0.660	-0.381	-0.371	-0.582	-0.509	-0.783	-0.296	0.532	-0.541	-0.009
6b-2	0.863	-0.440	-0.412	-0.586	-0.523	-0.667	-0.319	0.524	-0.892	-0.369
6c-1	0.651	-0.378	-0.373	-0.584	-0.502	-0.766	-0.284	0.535	-0.510	0.024
6c-2	0.861	-0.430	-0.411	-0.587	-0.520	-0.657	-0.282	0.522	-0.884	-0.362

Table S5-1 The WBIs in two HCl-interacted species **6** in MeCN.

Species	WBIs							
	V-O _b (1)	V-O _b (2)	V-O(3)	O(3)-H(1)	O(3)-H'	H-Cl(1)	H(2)-Cl(2)	V-Cl(1)
6a-1 + 2HCl	0.799	0.447	0.525	0.651	0.518	0.004	0.187	0.782
6a-2 + 2HCl	0.701	0.288	1.210	0.543	0.049	0.160	0.819	0.020
6b-1 + 2HCl	0.791	0.460	0.529	0.650	0.515	0.004	0.190	0.781
6b-2 + 2HCl	0.696	0.294	1.220	0.540	0.047	0.164	0.822	0.022
6c-1 + 2HCl	0.768	0.453	0.538	0.649	0.509	0.005	0.196	0.794
6c-2 + 2HCl	0.647	0.282	1.318	0.573		0.127	0.757	0.016

The H(2)-Cl(2) represents the first additional HCl that doesn't belong to species **6** itself. In the entry of O(3)-H', the H' represents H(2) for Cl-axial mode and H(3) for Cl-nonaxial mode. However, in **6c-2** + 2HCl (Fig. S10(d)), H(2) forms the hydrogen bond with Cl(1) rather than protonates O(3) or O_b(1).

Table S5-2 The natural charges in two HCl-interacted species **6** in MeCN.

Species	Natural charges									
	V	O _b (1)	O _b (2)	O(3)	O _t	H(1)	H(2)	Cl(1)	Cl(2)	HCl(1)
6a-1 + 2HCl	0.565	-0.591	-0.483	-0.875	-0.232	0.574	0.536	-0.409	-0.854	0.165
6a-2 + 2HCl	0.878	-0.621	-0.523	-0.739	-0.295	0.528	0.326	-0.872	-0.356	-0.344
6b-1 + 2HCl	0.563	-0.592	-0.445	-0.876	-0.220	0.574	0.535	-0.398	-0.850	0.176
6b-2 + 2HCl	0.876	-0.619	-0.527	-0.734	-0.292	0.526	0.325	-0.867	-0.340	-0.340
6c-1 + 2HCl	0.556	-0.589	-0.438	-0.873	-0.213	0.575	0.535	-0.385	-0.845	0.190
6c-2 + 2HCl	0.865	-0.632	-0.533	-0.670	-0.290	0.527	0.297	-0.775	-0.399	-0.247

Table S6 The ΔG_{298} between two kinds of coordination modes of species **6** in MeCN with and without two extra-interacted HCl.

	Species 6		Species 6 + 2HCl	
	G_{298} /a. u.	ΔG_{298} /kcal.mol ⁻¹	G_{298} /a. u.	ΔG_{298} /kcal.mol ⁻¹
6a-1	-1634.912061	15.867	-2556.471485	8.818
6a-2	-1634.937346		-2556.485538	
6b-1	-2554.064540	14.577	-3475.621886	8.705
6b-2	-2554.087770		-3475.635759	
6c-1	-3473.215213	13.828	-4394.770418	13.034
6c-2	-3473.237250		-4394.791189	

Table S7 The natural charges in the phenolic ring containing cleaved V-O_b bond in the two HCl-interacted species **6** in MeCN.

Species	Natural charges						
	O _b (2)	C(1)	C(2)	C(3)	C(4)	C(5)	C(6)
6a-1 + 2HCl	-0.483	0.485	0.186	-0.106	-0.079	-0.235	-0.196
6a-2 + 2HCl	-0.523	0.467	0.200	-0.106	-0.088	-0.239	-0.188
6b-1 + 2HCl	-0.445	0.473	0.189	-0.111	0.047	-0.228	-0.203
6b-2 + 2HCl	-0.527	0.474	0.204	-0.112	0.043	-0.233	-0.194
6c-1 + 2HCl	-0.438	0.470	0.186	-0.105	0.025	-0.186	-0.074
6c-2 + 2HCl	-0.533	0.479	0.201	-0.106	0.041	-0.255	-0.038

The atoms of specified species listed in Table S7 are in the same phenolic ring. The C(1) labeled in Fig. S10 is bonding to O_b(2), and other C atoms are arranged anticlockwise.

The distribution rule of natural charges in the dissociated phenolic ring of Cl-nonaxial mode (**6a-2** to **6c-2**) interacted with two HCl conforms to the description of visible spectral results (Fig. 6). Allowing for the high energy in Cl-axial mode (especially in **6c-1**), such a distribution rule is relatively reasonable, though the NC of O_b(2) in Cl-axial mode decreases with Cl substituting into the ligands (**6a-1** to **6c-1**).

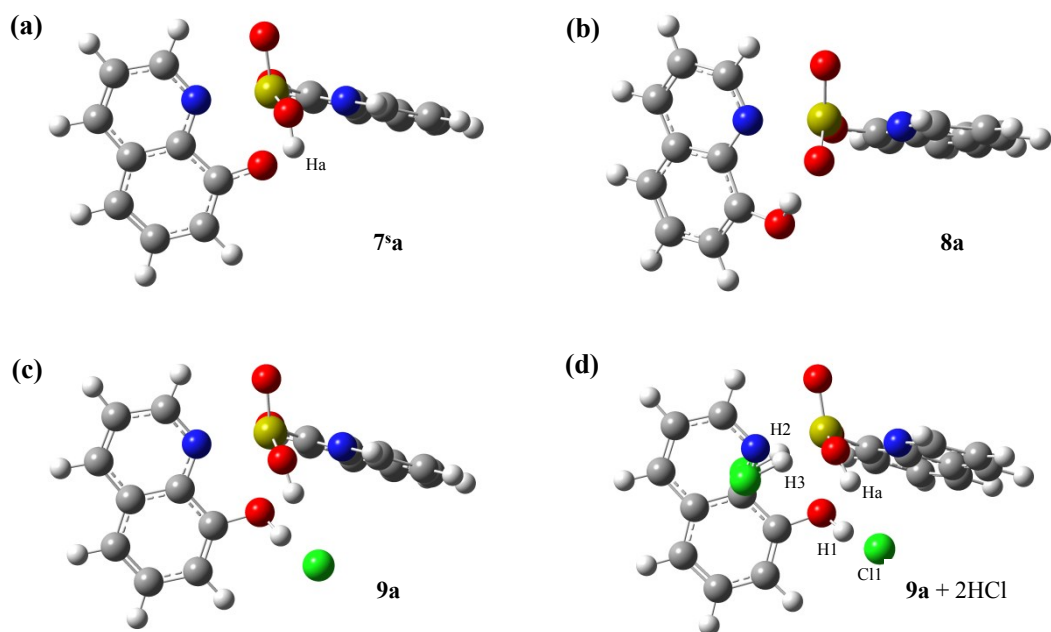


Fig. S11 Typical geometries of species **7^s** (a), **8** (b), **9** (c) and two-HCl-interacted **9** (d), and they are denoted as **7^{sa}**, **8a**, **9a** and **9a + 2HCl**, respectively.

Table S8-1 The WBIs in species **7^s** in MeCN.

Species	WBIs						
	V-N(1)	V-N(2)	V-O _b (1)	V-O _b (2)	V-O(3)	V=O _t	O(3)-Ha
7^{sa}	0.488	0.524	0.722	0.478	1.118	2.162	0.685
7^{sb}	0.480	0.513	0.707	0.473	1.106	2.110	0.691
7^{sc}	0.490	0.525	0.688	0.452	1.147	2.184	0.687

Table S8-2 The natural charges in species **7^s** in MeCN.

Species	Natural charges							
	V	N(1)	N(2)	O _b (1)	O _b (2)	O(3)	O _t	Ha
7^{sa}	0.836	-0.419	-0.411	-0.591	-0.685	-0.745	-0.338	0.533
7^{sb}	0.946	-0.428	-0.424	-0.600	-0.688	-0.736	-0.341	0.527
7^{sc}	0.839	-0.419	-0.416	-0.586	-0.673	-0.717	-0.310	0.531

Table S9-1 The WBIs in species **9** in MeCN.

Species	WBIs						
	V-O _b (1)	V-O _b (2)	V-O(3)	V=O _t	O _b (2)-H(1)	O(3)-Ha	Ha-Cl(1)
9a	0.782	0.218	1.222	2.216	0.538	0.615	0.082
9b	0.779	0.220	1.225	2.221	0.531	0.621	0.082
9c	0.735	0.212	1.256	2.230	0.522	0.607	0.098

Table S9-2 The natural charges in species **9** in MeCN.

Species	Natural charges							
	V	O _b (1)	O _b (2)	O(3)	O _t	Ha	H(1)	Cl(1)
9a	0.880	-0.580	-0.736	-0.718	-0.305	0.531	0.540	-0.827
9b	0.881	-0.576	-0.734	-0.704	-0.299	0.526	0.539	-0.821
9c	0.885	-0.581	-0.734	-0.691	-0.291	0.524	0.542	-0.809

Table S10-1 The WBIs in two HCl-interacted species **9** in MeCN.

Species	WBIs						
	V-O _b (1)	V-O _b (2)	V-O(3)	V=O _t	O _b (2)-H(1)	O(3)-Ha	Ha-Cl(1)
9a + 2HCl	0.725	0.225	1.146	2.242	0.538	0.590	0.104
9b + 2HCl	0.723	0.227	1.156	2.247	0.532	0.588	0.106
9c + 2HCl	0.705	0.224	1.178	2.253	0.515	0.583	0.113

Table S10-2 The natural charges in two HCl-interacted species **9** in MeCN.

Species	Natural charges							
	V	O _b (1)	O _b (2)	O(3)	O _t	Ha	H(1)	Cl(1)
9a + 2HCl	0.889	-0.614	-0.736	-0.759	-0.279	0.534	0.542	-0.812
9b + 2HCl	0.888	-0.611	-0.735	-0.753	-0.273	0.534	0.542	-0.805
9c + 2HCl	0.879	-0.612	-0.736	-0.743	-0.269	0.532	0.543	-0.793

Table S11 The ΔG_{298} between species **7^s** and **8**, and that between species **9** and the former ones (**7^s** or **8**) in MeCN.

Species	G ₂₉₈ /a. u.	ΔG_{298} /kcal.mol ⁻¹		
	Species 7^s , 8 or 9	7^s - 8	9 - 7^s - HCl	9 - 8 - HCl
7^sa	-1174.772869			
8a	-1174.767515	-3.360	-7.825	-11.185
9a	-1635.565703			
7^sb	-2093.925042			
8b	-2093.918577	-4.057	-5.991	-10.048
9b	-2554.714953			
7^sc	-3013.077521			
8c	-3013.066405	-6.975	-3.271	-10.246
9c	-3473.863097			

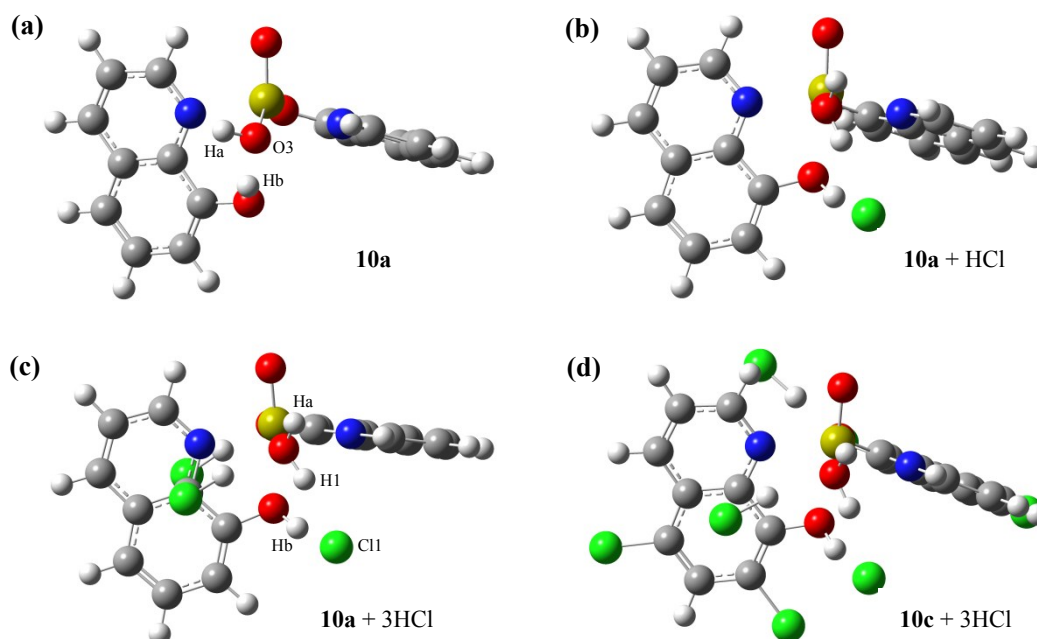
G₂₉₈(HCl in MeCN) = -460.780364.

The species **7^s** is more stable than **8**, and both of them can be transformed into **9** without an energy barrier under HCl interactions.

Table S12 The WBIs and natural charges in the HCl molecules that interacted with species **9**.

Species	WBIs				Natural charges			
	Original	+ 2HCl			Original	+ 2HCl		
	H(1)-Cl(1)	H(1)-Cl(1)	H(2)-Cl(2)	H(3)-Cl(3)	HCl(1)	HCl(1)	HCl(2)	HCl(3)
9a	0.155	0.152	0.824	0.842	-0.288	-0.269	-0.031	-0.020
9b	0.164	0.159	0.828	0.845	-0.282	-0.263	-0.029	-0.018
9c	0.164	0.169	0.835	0.849	-0.267	-0.250	-0.022	-0.005

The H(1)-Cl(1) belongs to species **9** (Fig. S11(c)), while H(2)-Cl(2) and H(3)-Cl(3) are additional HCl which protonate O_b(1) and O(3), respectively (Fig. S11(d)).

**Fig. S12** Typical geometries of **10a** (a), **10a** + HCl (b), **10a** + 3HCl (c) and **10c** + 3HCl (d).**Table S13-1** The WBIs in species **10** in MeCN.

Species	WBIs						
	V-O _b (1)	V-O _b (2)	V-O(3)	V=O _t	O(3)-Ha	O _b (2)-Hb	O(3)-Hb
10a	0.598	0.092	0.673	2.146	0.709	0.559	0.094
10b	0.591	0.103	0.670	2.156	0.714	0.553	0.096
10c	0.573	0.101	0.669	2.167	0.711	0.540	0.105

Table S13-2 The natural charges in species **10** in MeCN.

Species	Natural charges						
	V	O _b (1)	O _b (2)	O(3)	O _t	Ha	Hb
10a	0.914	-0.673	-0.770	-0.998	-0.479	0.524	0.562
10b	0.905	-0.669	-0.766	-0.973	-0.464	0.517	0.563
10c	0.911	-0.660	-0.756	-0.969	-0.453	0.519	0.566

Table S14 The WBIs in hydrogen bonded system containing H(1)-Cl(1) and species **10** in MeCN.

Species	+ HCl		+ 3HCl	
	Hb-Cl(1)	H(1)-Cl(1)	Hb-Cl(1)	H(1)-Cl(1)
10a	0.145	0.102	0.143	0.132
10b	0.151	0.108	0.150	0.132
10c	0.151	0.116	0.151	0.141

The H(1)-Cl(1) belongs to species **10** + HCl (Fig. S12(b)), while Hb-Cl(1) represents the hydrogen bond between Cl(1) and -O_b(2)Hb group.

The H(1)-Cl(1) bond is even weaker than this hydrogen bond, which further indicates the potential in the cleavage of the V^{IV}-OH₂ bond.

Table S15-1 The WBIs in one HCl-interacted species **10** in MeCN.

Species	WBIs						
	V-O _b (1)	V-O _b (2)	V-O(3)	V=O _t	O(3)-Ha	O _b (2)-Hb	O(3)-H(1)
10a + HCl	0.664	0.237	0.373	2.208	0.667	0.543	0.588
10b + HCl	0.654	0.229	0.382	2.219	0.671	0.539	0.590
10c + HCl	0.635	0.225	0.389	2.230	0.672	0.529	0.585

Table S15-2 The natural charges in one HCl-interacted species **10** in MeCN.

Species	Natural charges								
	V	O _b (1)	O _b (2)	O(3)	O _t	Ha	Hb	H(1)	Cl(1)
10a + HCl	0.888	-0.644	-0.735	-0.950	-0.424	0.570	0.544	0.551	-0.824
10b + HCl	0.888	-0.641	-0.736	-0.934	-0.406	0.566	0.543	0.545	-0.817
10c + HCl	0.891	-0.634	-0.734	-0.928	-0.399	0.565	0.546	0.542	-0.808

Table S16-1 The WBIs in three HCl-interacted species **10** in MeCN.

Species	WBIs						
	V-O _b (1)	V-O _b (2)	V-O(3)	V=O _t	O(3)-Ha	O _b (2)-Hb	O(3)-H(1)
10a + 3HCl	0.607	0.246	0.359	2.233	0.655	0.541	0.559
10b + 3HCl	0.605	0.246	0.361	2.239	0.654	0.535	0.558
10c + 3HCl	0.591	0.233	0.376	2.255	0.652	0.526	0.551

Table S16-2 The natural charges in three HCl-interacted species **10** in MeCN.

Species	Natural charges								
	V	O _b (1)	O _b (2)	O(3)	O _t	Ha	Hb	H(1)	Cl(1)
10a + 3HCl	0.891	-0.676	-0.739	-0.963	-0.401	0.580	0.547	0.550	-0.804
10b + 3HCl	0.891	-0.672	-0.738	-0.963	-0.394	0.580	0.547	0.550	-0.797
10c + 3HCl	0.886	-0.668	-0.738	-0.961	-0.383	0.582	0.549	0.549	-0.791

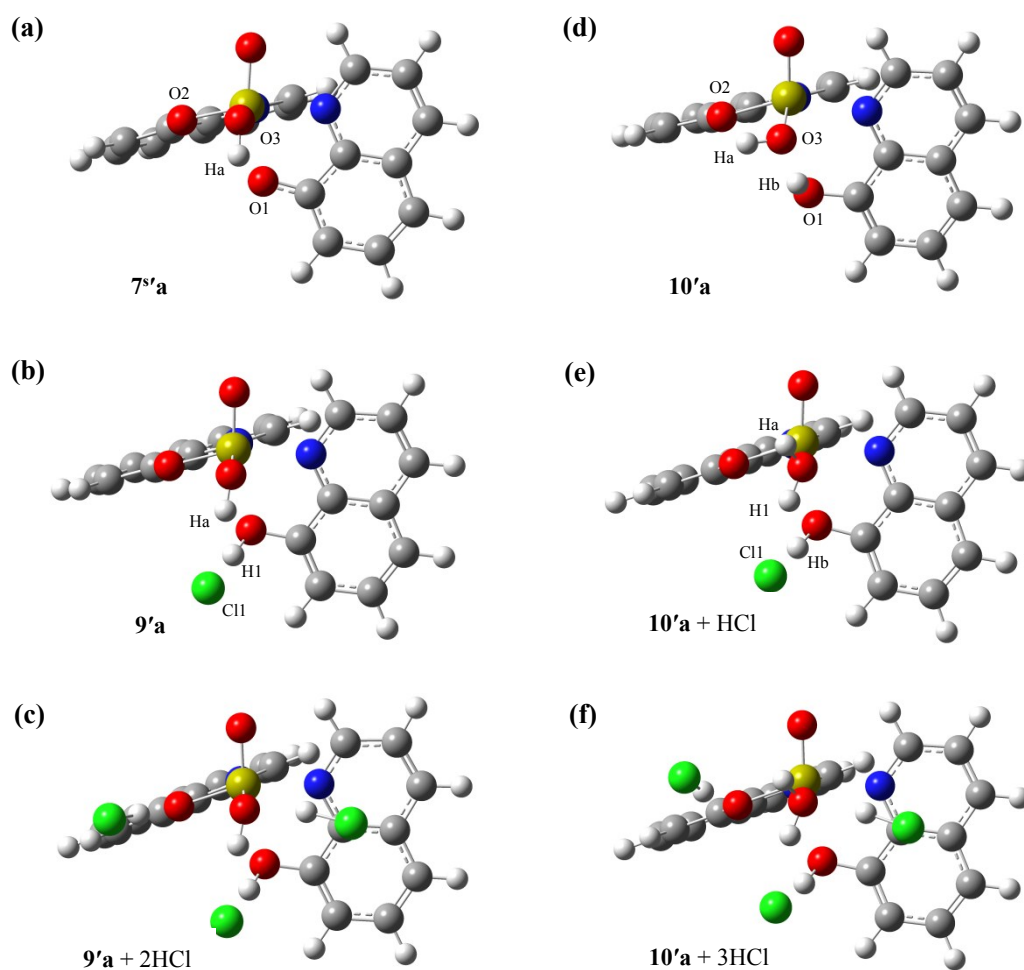


Fig. S13 Typical geometries of species $7^s\mathbf{a}$ (a), 9^a (b), $9^a + 2\text{HCl}$ (c), 10^a (d), $10^a + \text{HCl}$ (e) and $10^a + 3\text{HCl}$ (f), which are similar to the corresponding species without the superscript ($'$). The main difference is that $\text{V-O}_b(1)$ rather than $\text{V-O}_b(2)$ is cleaved in the species with a superscript.

Table S17 The ΔG_{298} between species 7^s and $7^{s'}$ in MeCN with and without interacted HCl.

	vanadic species		+ HCl		+ 3HCl	
	$G_{298}/\text{a. u.}$	$\Delta G_{298}/\text{kcal.mol}^{-1}$	$G_{298}/\text{a. u.}$	$\Delta G_{298}/\text{kcal.mol}^{-1}$	$G_{298}/\text{a. u.}$	$\Delta G_{298}/\text{kcal.mol}^{-1}$
$7^s\mathbf{a}$	-1174.772869	2.787	-1635.565703	0.213	-2557.112356	-1.394
$7^{s'}\mathbf{a}$	-1174.777311		-1635.566042		-2557.110135	
$7^s\mathbf{b}$	-2093.925042	2.654	-2554.714953	0.285	-3476.261202	-0.762
$7^{s'}\mathbf{b}$	-2093.929271		-2554.715407		-3476.259987	
$7^s\mathbf{c}$	-3013.077521	2.191	-3473.863097	-0.467	-4395.408876	-0.875
$7^{s'}\mathbf{c}$	-3013.081012		-3473.862352		-4395.407482	

Table S18 The WBIs and natural charges in the HCl molecules that interacted with species **9'**.

species	WBIs				Natural charges			
	Original	+ 2HCl			Original	+ 2HCl		
	H(1)-Cl(1)	H(1)-Cl(1)	H(2)-Cl(2)	H(3)-Cl(3)	HCl(1)	HCl(1)	HCl(2)	HCl(3)
9'a	0.161	0.160	0.844	0.829	-0.279	-0.262	-0.020	-0.032
9'b	0.171	0.169	0.848	0.835	-0.272	-0.255	-0.017	-0.029
9'c	0.176	0.171	0.848	0.852	-0.259	-0.241	-0.016	-0.019

Table S18 shows the similar variational rule to Table S12.

Table S19 The ΔG_{298} between species **10** and **10'** in MeCN with and without interacted HCl.

	vanadic species		+ HCl		+ 3HCl	
	$G_{298}/\text{a. u.}$	$\Delta G_{298}/\text{kcal.mol}^{-1}$	$G_{298}/\text{a. u.}$	$\Delta G_{298}/\text{kcal.mol}^{-1}$	$G_{298}/\text{a. u.}$	$\Delta G_{298}/\text{kcal.mol}^{-1}$
10a	-1175.370360	0.479	-1636.177321	0.208	-2557.725807	-0.066
10'a	-1175.371124		-1636.177653		-2557.725702	
10b	-2094.521871	0.149	-2555.328406	-0.006	-3476.875540	-0.700
10'b	-2094.522109		-2555.328396		-3476.874425	
10c	-3013.672257	-0.490	-3474.475619	0.403	-4396.021025	0.763
10'c	-3013.671476		-3474.476262		-4396.022241	

The reaction pathway containing species **7's** and **10** has certain advantages according to Tables S17 and S19.

References

1. M. J. Frisch, et al., *Gaussian 09, Revision D.01*, Gaussian Inc., Wallingford, CT, 2013.
2. Y. Zhao and D. G. Truhlar, *Theor. Chem. Account.*, 2008, **120**, 215.
3. P. J. Hay and W. R. Wadt, *J. Chem. Phys.*, 1985, **82**, 270.
4. P. J. Hay and W. R. Wadt, *J. Chem. Phys.*, 1985, **82**, 299.
5. A. W. Ehlers, M. Böhme, S. Dapprich, A. Gobbi, A. Höllwarth, V. Jonas, K. F. Köhler, R. Stegmann, A. Veldkamp and G. Frenking, *Chem. Phys. Lett.*, 1993, **208**, 111.
6. L. E. Roy, P. J. Hay and R. L. Martin, *J. Chem. Theory Comput.*, 2008, **4**, 1029.
7. K. L. Schuchardt, B. T. Didier, T. Elsethagen, L. Sun, V. Gurumoorthi, J. Chase, J. Li and T. L. Windus, *J. Chem. Inf. Model.*, 2007, **47**, 1045.
8. S. E. Wheeler and K. N. Houk, *J. Chem. Theory Comput.*, 2010, **6**, 395.
9. G. Scalmani and M. J. Frisch, *J. Chem. Phys.*, 2010, **132**, 114110.
10. F. Weinhold and C. R. Landis, *Valency and Bonding: A Natural Bond Orbital Donor-Acceptor Perspective*, Cambridge University Press, Cambridge, 2005.

11. G. Beamson and D. Briggs, *High Resolution XPS of Organic Polymers: The Scienta ESCA300 Database*, Wiley, Chichester, 1992.
12. X. Chen, B. Zhao, Y. Cai, M. O. Tade and Z. Shao, *Nanoscale*, 2013, **5**, 12589.
13. K. Tang, Y. Li, H. Cao, F. Duan, Y. Zhang and Y. Wang, *RSC Adv.*, 2015, **5**, 40163.
14. C. R. Waidmann, A. G. DiPasquale and J. M. Mayer, *Inorg. Chem.*, 2010, **49**, 2383.
15. I. Gryca, K. Czerwińska, B. Machura, A. Chrobok, L. S. Shul'pina, M. L. Kuznetsov, D. S. Nesterov, Y. N. Kozlov, A. J. L. Pombeiro, I. A. Varyan, and G. B. Shul'pin, *Inorg. Chem.*, 2018, **57**, 1824.